DNA Nanotechnology

DOI: 10.1002/anie.201410895

Gold-Nanoparticle-Mediated Jigsaw-Puzzle-like Assembly of Supersized Plasmonic DNA Origami**

*Guangbao Yao, Jiang Li, Jie Chao, Hao Pei, Huajie Liu, Yun Zhao, Jiye Shi, Qing Huang, Lianhui Wang, Wei Huang, and Chunhai Fan**

Abstract: *DNA origami has rapidly emerged as a powerful and programmable method to construct functional nanostructures. However, the size limitation of approximately 100 nm in classic DNA origami hampers its plasmonic applications. Herein, we report a jigsaw-puzzle-like assembly strategy mediated by gold nanoparticles (AuNPs) to break the size limitation of DNA origami. We demonstrated that oligonucleotide-functionalized AuNPs function as universal joint units for the one-pot assembly of parent DNA origami of triangular shape to form sub-microscale super-origami nanostructures. AuNPs anchored at predefined positions of the super-origami exhibited strong interparticle plasmonic coupling. This AuNP-mediated strategy offers new opportunities to drive macroscopic self-assembly and to fabricate well-defined nanophotonic materials and devices.*

Biomolecules are dynamically organized in cells with spatial and temporal orderliness to realize their physiological functions. Such elegant supramolecular assembly has inspired researchers to create molecular/biomolecular structures with dynamic organization outside of cells. One promising approach is to exploit the simple Watson–Crick base-pairing principle to drive self-assembly of nucleic acids and even inorganic nanoparticles in solution.[1] The invention of DNA origami by Rothemund facilitated the creation of large and complex DNA nanostructures with uniform geometries and finite sizes.[2] In a typical DNA origami assembly process, a long M13 viral single-stranded DNA template is hybridized with hundreds of computer-designed sequence-specific short staple DNA strands to fold into predefined 1D, 2D, or 3D nanostructures. These DNA origami nanostructures have found numerous applications in single-molecule biophysical studies,[3] biomolecular assays,[4] drug delivery,[5] and in enzyme cascades.[6]

Nevertheless, it remains a hurdle to assemble higher-order structures that exceed the size limitation of M13 viral genomic-DNA-based origami (typically < 150 nm, and molecular weight < 50 MDa). More recently, several groups have designed supersized origami (super-origami) structures using longer-template or sticky-end assembly.[7] It is also desirable to endow DNA origami with notable optical properties that are absent in DNA molecules.[8] To address this problem, significant efforts have been made to decorate DNA origami with metal or semiconductor nanoparticles.[9] By exploiting the site-specific addressability of DNA origami, several groups have fabricated a range of DNA-based nanophotonic materials[10] or even plasmonic metamaterials[11] that exhibit unique plasmonic chirality,[10] metal-enhanced fluorescence,[12] and surface-enhanced Raman scattering (SERS).[13]

Herein, we devise a straightforward and versatile strategy to construct plasmonic super-origami nanostructures by employing DNA-modified gold nanoparticles (DNA–AuNPs) to assemble individual origami triangles like a jigsaw puzzle. Although AuNPs modified with a dense layer of thiolated oligonucleotides have proven to drive self-assembly even to form macroscopic crystals, they typically lack the ability to form structures with finite sizes. Additionally, unlike previous DNA self-assembly approaches that rely on using one-to-one sticky-end DNA fragments, we exploit the multivalent binding ability of DNA–AuNPs which acts as a universal joint to organize jigsaw-like origami pieces. More significantly, these inorganic AuNPs are incorporated in the super-origami during the one-pot assembly process, generating plasmonic DNA nanostructures without subsequent modification.

To demonstrate our AuNP-mediated jigsaw-puzzle-like assembly strategy, we employed triangular DNA origami and DNA–AuNPs as two building blocks to form DNA super-origami nanostructures (Figure 1b). The triangular origami was assembled using M13 and staple strands,[2] with several joint strands stretched out at different positions. These joint strands are fully complementary to the dense, thiolated oligonucleotide strands bound to AuNPs (10 nm in diameter).

[*] G. Yao,[+] Prof. Y. Zhao
Key Laboratory of Bio-Resources and Eco-Environment
Ministry of Education, College of Life Sciences
Sichuan University, Chengdu 610064 (China)
G. Yao,[+] Dr. J. Li,[+] Dr. H. Pei, Dr. H. Liu, Dr. J. Shi, Dr. Q. Huang, Prof. C. Fan
Division of Physical Biology and Bioimaging Center
Shanghai Synchrotron Radiation Facility
CAS Key Laboratory of Interfacial Physics and Technology
Shanghai Institute of Applied Physics
Chinese Academy of Sciences, Shanghai 201800 (China)
E-mail: fchh@sinap.ac.cn
Dr. J. Chao,[+] Prof. L. Wang, Prof. W. Huang
Institute of Advanced Materials, Nanjing University of Posts and Telecommunications, Nanjing 210003 (China)
Dr. J. Shi
UCB Pharma, 208 Bath Road, Slough SL1 3WE (UK)
[+] These authors contributed equally to this work.

[**] This work was financially supported by the National Basic Research Program (973 Program grant numbers 2013CB932803, 2013CB825800, 2013CB932803, and 2012CB932600) and the NSFC (grant numbers 91313302, 21390414, 21422508, 21305151, 21329501, 213051051, and 91123037).

Supporting information for this article is available on the WWW under http://dx.doi.org/10.1002/anie.201410895.

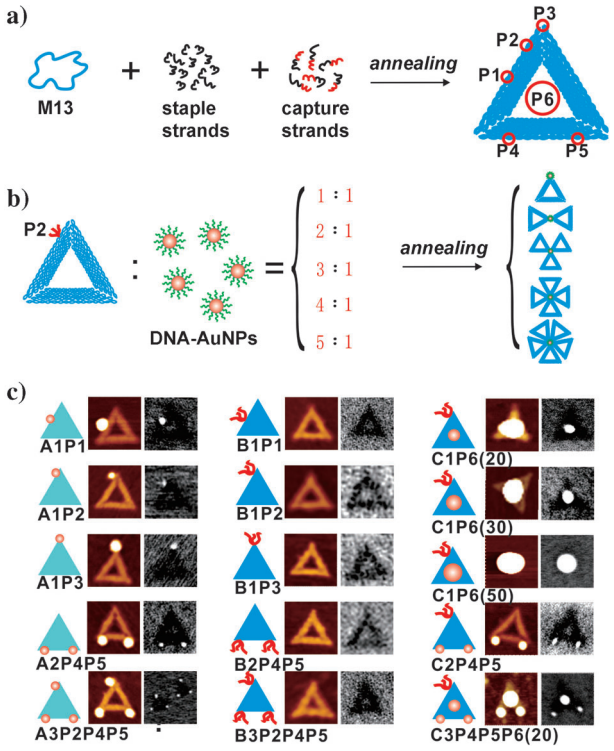

Figure 1. Schematic representation of AuNP-mediated jigsaw-puzzle-like assembly of super-origami. a) The assembly of triangular origami showing the specific anchoring positions (P1–P6) for AuNPs. b) The assembly of flower-like super-origami. c) AFM and SEM images and representative structures of triangular DNA origami with different numbers of AuNPs (represented by orange spheres) at different positions. In series A (left column), the triangular origami is anchored with one to three 10 nm AuNPs, with the number after A indicating the number of AuNPs. For example, structure A1P1 has one AuNP at position P1. Series B is the AuNP-free counterpart of series A. In series C, the centroid position P6 is occupied by AuNPs of different sizes (20, 30, and 50 nm; NP size given in parentheses) with the exception of C2P4P5 where P6 is vacant. In C3, P4 and P5 are bound to AuNPs (10 nm) and P2 is vacant. Vacant binding sites are denoted by a red symbol.

DNA–AuNPs can be anchored at six specific positions on the triangular origami, denoted P1–P6 (Figure 1a; Figure S9 in the Supporting Information), each of which has three DNA joint strands stretched out (with the exception of P6). These positions fall into four classes depending on the location of the position on the DNA origami triangle: a) edge middle (P1), b) 15 nm away from the vertex (P2, P4, P5), c) vertices (P3), and d) centroid (P6). By combining different numbers and sizes of AuNPs at these predefined positions, three series of nanostructures, namely A, B, and C, were prepared (Figure 1c). Each of the nanostructures could be readily formed in solution with high yield (>90%). Both atomic force microscope (AFM) and scanning electron microscope (SEM) confirmed the formation of well-defined AuNP-anchored triangular origami nanostructures (Figure 1c and Figure S1), paving the way for the use of AuNPs as universal joints for jigsaw-puzzle-like assembly of super-origami.

We studied the positional effect of the AuNP on super-origami assembly using triangular origami from series A and B. When AuNPs were anchored in the middle of the edge (P1), the formation of arrow-shaped super-origami was observed, with a maximum number of three origami triangles (Figure 2a). Moving AuNPs down to P2 increased the maximum origami number to five (Figure 2a). When AuNPs were positioned at the P3 vertex, we obtained a nearly perfect hexagonal-shaped flower-like nanostructure with six origami triangles (Figure 2a and Figure S2). Clearly, this positional effect largely arises from the steric hindrance, with the vertex position P3 having the greatest capacity for hybridization-based assembly.

To assemble super-origami using DNA–AuNPs, we mixed B1P2-type triangular origami and DNA–AuNPs in solution at different molar ratios (origami/DNA–AuNP from 1:5 to 10:1). Gel electrophoresis and AFM confirmed the formation of DNA super-origami nanostructures (Figure 2b,c; Figure S3). We found that the super-origami assembly is strongly dependent on stoichiometry, resulting in the formation of flower-like nanostructures with 1–5 triangular origami "petals". When DNA–AuNPs are in large excess (origami/DNA–AuNP = 1:5), we obtained almost exclusively "single-petal" nanostructures, that is, with one origami triangle linked with one AuNP, with a very high yield of 98%. With increasing ratio of origami/DNA–AuNP, the yield of "single-petal" nanostructures decreases and "multi-petal" nanostructures composed of two to five origami triangles are formed (see the changes in nanostructure distribution with increasing ratio in Figure 2b). At an origami/DNA–AuNP ratio of 10:1, primarily five-petal super-origami flower nanostructures were formed with a yield of 87% (excess unbound triangular origami are not counted, see Table S1). Notably, no six-petal nanostructures could be detected, likely as a result of steric hindrance (see above). Thus, the jigsaw-puzzle-like assembly of super-origami can be well controlled by tuning the stoichiometry. Further studies demonstrated that replacement of 10 nm AuNPs with smaller (5 nm) or larger (20 nm) AuNPs could similarly control the super-origami assembly (Figure S4).

Having demonstrated the jigsaw-puzzle assembly strategy for super-origami using AuNPs as the universal joint unit, we further explored the assembly of higher-order super-origami nanostructures using different series of triangular origami (shown in Figure 1c) and multiple AuNP joints. By mixing series A and series B origami triangles in solution, a wide range of assembly combinations were detected using AFM imaging (Figure 3). As expected, the combination of A1 and B1 led to the formation of flower-like super-origami with different number of petals, similar to the case of AuNP-mediated assembly of triangular origami (Figure 2b,c). When the number of AuNPs was increased to two or three (A2 or A3) and mixed with B1, higher-order jigsaw-puzzle-like assembly was detected with up to nine origami triangles. In these nanostructures, A2 or A3 are surrounded by B1 origami triangles. Interestingly, when A2 or A3 were mixed with B2, which has two binding sites, we obtained super-origami nanostructures with regular diamond or trapezoid shapes, possibly because of the increased binding ability of the multivalent origami triangles. Further increasing the number of binding sites to three by using B3 did not result in

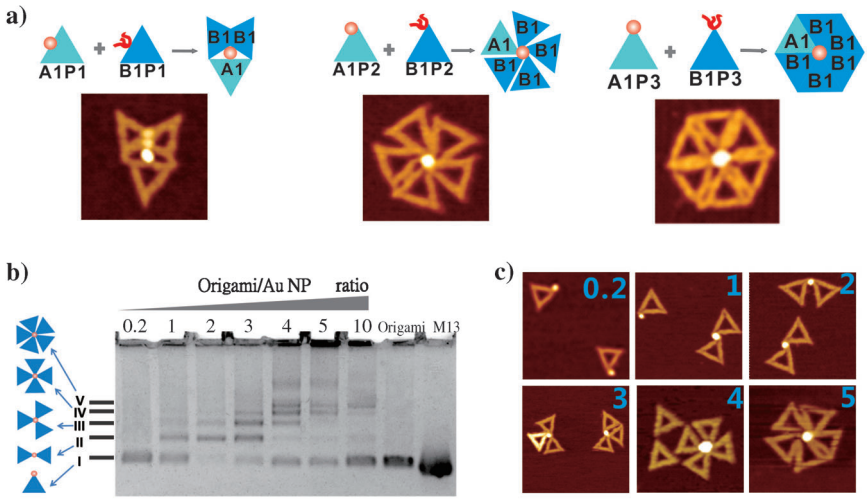

Figure 2. Positional and stoichiometric effects in super-origami assembly. a) Schematic representation and AFM images of super-origami structures derived from A1 and B1 origami triangles with different anchoring positions. b) Gel electrophoresis of super-origami, with I–V denoting flower-like nanostructures with 1–5 origami triangles. c) AFM images showing the super-origami nanostructures formed at different origami/DNA–AuNP ratios.

controllable super-origami assembly. In contrast, we observed the formation of irregular 2D architectures, with a representative image shown in Figure 3 (A3 + B3).

The ability to assemble well-defined super-origami nanostructures using AuNPs prompted us to study their plasmonic properties. Indeed, the size of the triangular origami (125 nm) has been doubled in the hexagonal nanostructure (250 nm) or even multiplied in some complex nanostructures (up to 400 nm), providing significantly more space to fabricate nanophotonic devices. However, the 10 nm AuNPs employed in the super-origami do not exhibit prominent plasmonic properties. To address this problem, we loaded larger AuNPs in the cavity of the triangular origami from series C. We demonstrated that these AuNPs could similarly control the formation of super-origami nanostructures using a jigsaw-puzzle-like assembly process. By mixing C series origami with AuNPs (20 nm) at the centroid and with DNA-AuNPs (10 nm) at the joints, we constructed a range of "planet–satellite" nanostructures with different numbers of AuNPs (Figure S8a–c).

We investigated the plasmonic properties of super-origami containing 50 nm AuNPs. These systems show high surface plasmon resonance (SPR) absorption and readily detectable scattering under the dark-field microscope (DFM). We assembled three types of super-origami nanostructures with two, three, and four AuNPs (Figure S8d, 50 nm versus 20 nm AuNPs in ratios of 1:1, 2:1, and 3:1). Super-origami nanostructures obtained using this method were transferred onto indium tin oxide (ITO) substrates. Single-particle DFM spectra on individual super-origami were collected with the assistance of ex situ SEM (Figure S6). The scattering spectrum for a single-petal nanostructure displayed a SPR absorption maximum at $\lambda =$ 560 nm, which is similar to that for a single 50 nm AuNP (Figure S7A). This indicates that 20 nm AuNPs are too small to alter the plasmonic properties of 50 nm AuNPs at this distance. The two-petal nanostructure exhibited a red-shifted SRP absorption band at $\lambda = 580$ nm, suggesting surface plasmon coupling between the two 50 nm AuNPs and the center 20 nm AuNPs. Furthermore, the scattering spectrum for the three-petal nanostructure showed the appearance of two bands at $\lambda = 570$ nm and $\lambda = 680$ nm, which could arise

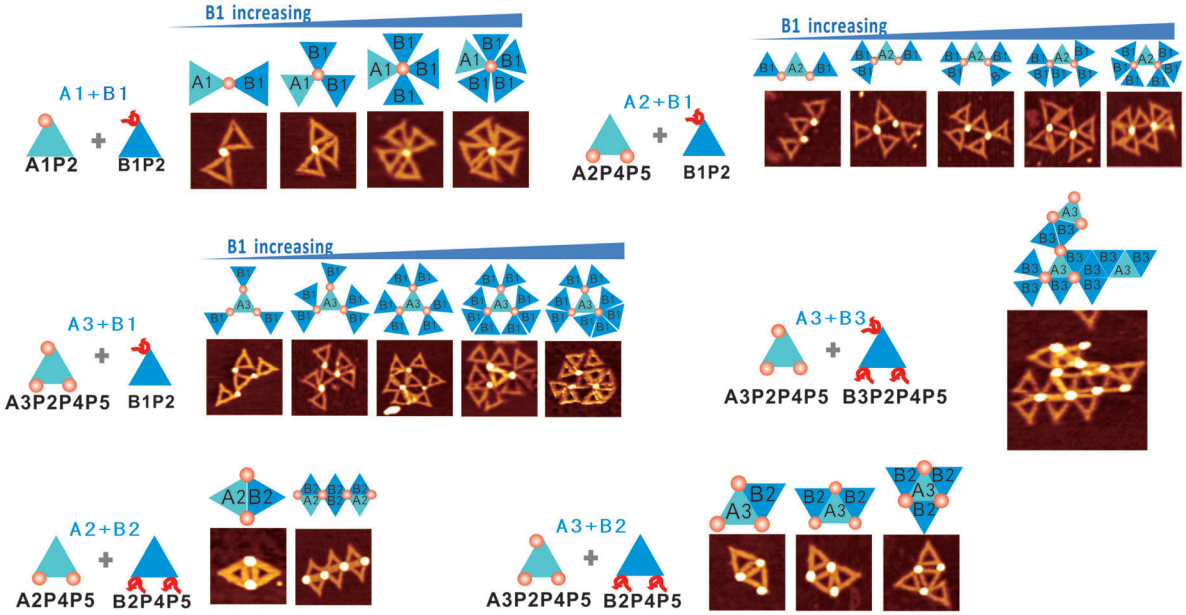

Figure 3. Jigsaw-puzzle-like assembly of higher-order super-origami nanostructures using triangular origami from series A and B.

from asymmetric surface plasmonic coupling between AuNPs. This result was supported by SEM which showed that the three petals are largely asymmetric in shape.

In summary, we have introduced a general new strategy to assemble jigsaw-like super-origami that relies on AuNP-based universal joints rather than DNA sticky ends. By using this strategy, we have obtained a range of supersized DNA origami with higher-order nanostructures. The largest nanostructure comprises more than ten DNA origami triangles, with the overall size reaching almost the micrometer scale and the molecular weight over 50 MDa. In addition to breaking the size limitation of DNA origami, this AuNP-based super-origami strategy has several additional advantages. First, AuNPs with plasmonic properties are inherently embedded in assembled nanostructures with precisely controlled interparticle distance. As a result, these nanostructures should have significant potential in nanophotonic applications including in biosensors, biomedicine, and in energy harvesting. Second, this AuNP-mediated super-origami assembly combines the precise controllability of assembly based on DNA sticky ends and the flexibility of DNA–AuNP-based multivalent assembly, facilitating the jigsaw-puzzle-like organization of DNA origami into uniform geometries and finite sizes. Third, the use of AuNPs as universal joints provides a general approach for DNA self-assembly and may also be extended to the assembly of various types of biomolecules including aptamers and proteins.

Received: November 10, 2014
Revised: December 31, 2014
Published online: January 22, 2015

Keywords: DNA origami · gold · nanoparticles · nanostructures · self-assembly

[1] a) N. C. Seeman, *J. Theor. Biol.* **1982**, *99*, 237 – 247; b) F. A. Aldaye, A. L. Palmer, H. F. Sleiman, *Science* **2008**, *321*, 1795 – 1799; c) P. K. Lo, P. Karam, F. A. Aldaye, C. K. McLaughlin, G. D. Hamblin, G. Cosa, H. F. Sleiman, *Nat. Chem.* **2010**, *2*, 319 – 328.

[2] P. W. K. Rothemund, *Nature* **2006**, *440*, 297 – 302.

[3] a) A. Kuzuya, M. Kimura, K. Numajiri, N. Koshi, T. Ohnishi, F. Okada, M. Komiyama, *ChemBioChem* **2009**, *10*, 1811 – 1815; b) N. D. Derr, B. S. Goodman, R. Jungmann, A. E. Leschziner, W. M. Shih, S. L. Reck-Peterson, *Science* **2012**, *338*, 662 – 665.

[4] D. Koirala, P. Shrestha, T. Emura, K. Hidaka, S. Mandal, M. Endo, H. Sugiyama, H. Mao, *Angew. Chem. Int. Ed.* **2014**, *53*, 8137 – 8141; *Angew. Chem.* **2014**, *126*, 8275 – 8279.

[5] V. J. Schüller, S. Heidegger, N. Sandholzer, P. C. Nickels, N. A. Suhartha, S. Endres, C. Bourquin, T. Liedl, *ACS Nano* **2011**, *5*, 9696 – 9702.

[6] a) O. I. Wilner, Y. Weizmann, R. Gill, O. Lioubashevski, R. Freeman, I. Willner, *Nat. Nanotechnol.* **2009**, *4*, 249 – 254; b) J. Fu, M. Liu, Y. Liu, N. W. Woodbury, H. Yan, *J. Am. Chem. Soc.* **2012**, *134*, 5516 – 5519; c) Y. Fu, D. Zeng, J. Chao, Y. Jin, Z. Zhang, H. Liu, D. Li, H. Ma, Q. Huang, K. V. Gothelf, C. Fan, *J. Am. Chem. Soc.* **2013**, *135*, 696 – 702; d) J. Fu, Y. R. Yang, A. Johnson-Buck, M. Liu, Y. Liu, N. G. Walter, N. W. Woodbury, H. Yan, *Nat. Nanotechnol.* **2014**, *9*, 531 – 536.

[7] a) R. J. Kershner, L. D. Bozano, C. M. Micheel, A. M. Hung, A. R. Fornof, J. N. Cha, C. T. Rettner, M. Bersani, J. Frommer, P. W. K. Rothemund, G. M. Wallraff, *Nat. Nanotechnol.* **2009**, *4*, 557 – 561; b) A. Rajendran, M. Endo, Y. Katsuda, K. Hidaka, H. Sugiyama, *ACS Nano* **2011**, *5*, 665 – 671; c) Z. Zhao, H. Yan, Y. Liu, *Angew. Chem. Int. Ed.* **2010**, *49*, 1414 – 1417; *Angew. Chem.* **2010**, *122*, 1456 – 1459; d) W. Liu, H. Zhong, R. Wang, N. C. Seeman, *Angew. Chem. Int. Ed.* **2011**, *50*, 264 – 267; *Angew. Chem.* **2011**, *123*, 278 – 281; e) Z. Zhao, Y. Liu, H. Yan, *Nano Lett.* **2011**, *11*, 2997 – 3002; f) A. Aghebat Rafat, T. Pirzer, M. B. Scheible, A. Kostina, F. C. Simmel, *Angew. Chem. Int. Ed.* **2014**, *53*, 7665 – 7668; *Angew. Chem.* **2014**, *126*, 7797 – 7801.

[8] a) F. A. Aldaye, H. F. Sleiman, *Angew. Chem. Int. Ed.* **2006**, *45*, 2204 – 2209; *Angew. Chem.* **2006**, *118*, 2262 – 2267; b) F. A. Aldaye, H. F. Sleiman, *J. Am. Chem. Soc.* **2007**, *129*, 4130 – 4131; c) M. Pilo-Pais, S. Goldberg, E. Samano, T. H. Labean, G. Finkelstein, *Nano Lett.* **2011**, *11*, 3489 – 3492; d) J. Elbaz, A. Cecconello, Z. Fan, A. O. Govorov, I. Willner, *Nat. Commun.* **2013**, *4*, 2000; e) S. Shimron, A. Cecconello, C.-H. Lu, I. Willner, *Nano Lett.* **2013**, *13*, 3791 – 3795; f) A. P. Eskelinen, R. J. Moerland, M. A. Kostiainen, P. Torma, *Small* **2014**, *10*, 1057 – 1062; g) R. Schreiber, J. Do, E.-M. Roller, T. Zhang, V. J. Schuller, P. C. Nickels, J. Feldmann, T. Liedl, *Nat. Nanotechnol.* **2014**, *9*, 74 – 78; h) X. Liu, C.-H. Lu, I. Willner, *Acc. Chem. Res.* **2014**, *47*, 1673 – 1680.

[9] a) B. Ding, Z. Deng, H. Yan, S. Cabrini, R. N. Zuckermann, J. Bokor, *J. Am. Chem. Soc.* **2010**, *132*, 3248 – 3249; b) S. Pal, Z. Deng, B. Ding, H. Yan, Y. Liu, *Angew. Chem. Int. Ed.* **2010**, *49*, 2700 – 2704; *Angew. Chem.* **2010**, *122*, 2760 – 2764; c) S. Pal, Z. Deng, H. Wang, S. Zou, Y. Liu, H. Yan, *J. Am. Chem. Soc.* **2011**, *133*, 17606 – 17609; d) Z. Deng, A. Samanta, J. Nangreave, H. Yan, Y. Liu, *J. Am. Chem. Soc.* **2012**, *134*, 17424 – 17427.

[10] a) A. Kuzyk, R. Schreiber, Z. Fan, G. Pardatscher, E.-M. Roller, A. Hoegele, F. C. Simmel, A. O. Govorov, T. Liedl, *Nature* **2012**, *483*, 311 – 314; b) X. Shen, C. Song, J. Wang, D. Shi, Z. Wang, N. Liu, B. Ding, *J. Am. Chem. Soc.* **2012**, *134*, 146 – 149; c) R. Schreiber, N. Luong, Z. Fan, A. Kuzyk, P. C. Nickels, T. Zhang, D. M. Smith, B. Yurke, W. Kuang, A. O. Govorov, T. Liedl, *Nat. Commun.* **2013**, *4*, 2948; d) X. Lan, Z. Chen, G. Dai, X. Lu, W. Ni, Q. Wang, *J. Am. Chem. Soc.* **2013**, *135*, 11441 – 11444.

[11] A. Kuzyk, R. Schreiber, H. Zhang, A. O. Govorov, T. Liedl, N. Liu, *Nat. Mater.* **2014**, *13*, 862 – 866.

[12] G. P. Acuna, F. M. Moller, P. Holzmeister, S. Beater, B. Lalkens, P. Tinnefeld, *Science* **2012**, *338*, 506 – 510.

[13] a) P. Kühler, E. M. Roller, R. Schreiber, T. Liedl, T. Lohmuller, J. Feldmann, *Nano Lett.* **2014**, *14*, 2914 – 2919; b) M. Pilo-Pais, A. Watson, S. Demers, T. H. LaBean, G. Finkelstein, *Nano Lett.* **2014**, *14*, 2099 – 2104.

